

Measurement of NaCl/Ge(001) interface states by inelastic low-energy electron scattering with high momentum resolution

V. Zielasek,* T. Hildebrandt, and M. Henzler

Institut für Festkörperphysik, Universität Hannover, Appelstrasse 2, D-30167 Hannover, Germany

(Received 30 June 2003; revised manuscript received 8 December 2003; published 21 May 2004)

Only a few techniques render possible to study properties of buried interfaces. Among them is electron energy loss spectroscopy, which can provide information about vibrational or electronic interface excitations via their long-range electromagnetic fields penetrating the covering film. For a scattering geometry close to normal incidence, we present a high-resolution experimental analysis of the angular distribution of low-energy electrons scattered inelastically at epitaxial NaCl layers on Ge(001). Our analysis unequivocally separates scattering due to NaCl surface defects from scattering due to substrate electronic excitations in the same energy range. In agreement with dipole scattering theory, we find the width of the angular distribution of scattering at excitations of the buried interface directly related to the thickness of the covering film, enabling us to localize the causative electronic transitions with respect to the surface normal. We identify energy losses due to interband transitions involving Ge bulk and interface states, respectively, providing evidence that the dimerization of the Ge surface is not removed after NaCl deposition.

DOI: 10.1103/PhysRevB.69.205313

PACS number(s): 61.14.-x, 73.20.-r, 71.36.+c

I. INTRODUCTION

Electron energy loss spectroscopy (EELS) in connection with the dielectric theory is a powerful tool for the analysis of multilayered surface structures.^{1,2} In the small-angle scattering regime the electrons interact with elementary excitations of the surface and underlying interfaces mainly via polarization fields set up in the vacuum above the surface (dipole scattering). Consequently, the probing depth depends on the range of dipolar fields within the layered surface which may well exceed the range of low-energy electrons penetrating the surface. Computations of energy loss spectra which treat the surface as a layered dielectric³ are in satisfactory agreement with experimental results as demonstrated by a number of successful studies, e.g., for phonon and plasmon polariton modes of semiconductor superlattices,^{4,5} semiconductor space-charge layers,⁶ δ -doped layers,⁷ and insulating thin films.⁸ Typically, the experimental results comprise electron energy loss spectra measured for some fixed scattering conditions, sampling the dispersion relation of the surface and interface modes at few selected points in the surface Brillouin zone (SBZ). The identification of surface or interface modes based on this approach is unpromising in the regime of interband transitions where high damping results in broad energy loss features that hamper detection of any dispersion. In addition, excitations localized in different layers but contributing to energy loss features in close-by energy range may be misleading.

Here we present a high-resolution experimental study of the angular distribution of inelastic low-energy electron scattering at epitaxial NaCl layers on Ge(001). Scattering profiles that encompass the entire SBZ around the specular reflection were obtained for selected energy losses by using a scattering geometry close to normal incidence. The range of selected energy losses covers Ge interband transitions with energies below the NaCl band gap. Analyzing the scattering

profiles within the dipole scattering theory as outlined in the following allows us to locate elementary excitations within the layered surface and identify surface or interface modes.

For more than a decade NaCl films on Ge(001) have served as a model system for epitaxial insulating thin films,^{9,10} displaying, e.g., the so-called “carpet growth mode”¹¹ and various types of surface color centers that determine the chemical reactivity of the surface.^{12–14} The NaCl/Ge(001) interface plays an important role for the growth mode and seems to affect the color center generation or stability in the film. In this paper the detection of electronic states located at the interface of up to 20 ML (where ML stands for monolayer) thick NaCl films on Ge(001) is presented, providing evidence that the dimerization of the Ge(001) surface is not removed at the NaCl/Ge interface. The experimental analysis clearly separates dipole scattering due to electronic transitions in the Ge substrate from inelastic scattering due to surface color centers of the NaCl capping layer while both types of excitations exhibit similar features in energy loss spectra without momentum resolution.

II. EXPERIMENT

The experiments were performed in ultrahigh vacuum (basic pressure below 10^{-8} Pa) using energy loss spectroscopy of low-energy electron diffraction (ELS-LEED).¹⁵ With the scattering geometry being instrumentally fixed to near-normal incidence (about 6° off normal) the ELS-LEED achieves a transfer width of 150 nm at an energy of 100 eV, corresponding to a momentum resolution of 0.042 nm^{-1} with respect to the surface component of the scattering vector and an angular resolution better than 0.05° . For maximum loss intensity the energy resolution was set to 60 meV full width at half maximum.

We studied layers of NaCl with thicknesses up to 5.6 nm corresponding to 20 ML, which grow epitaxially on Ge(001) surfaces. Charging of the insulator surface by the measuring

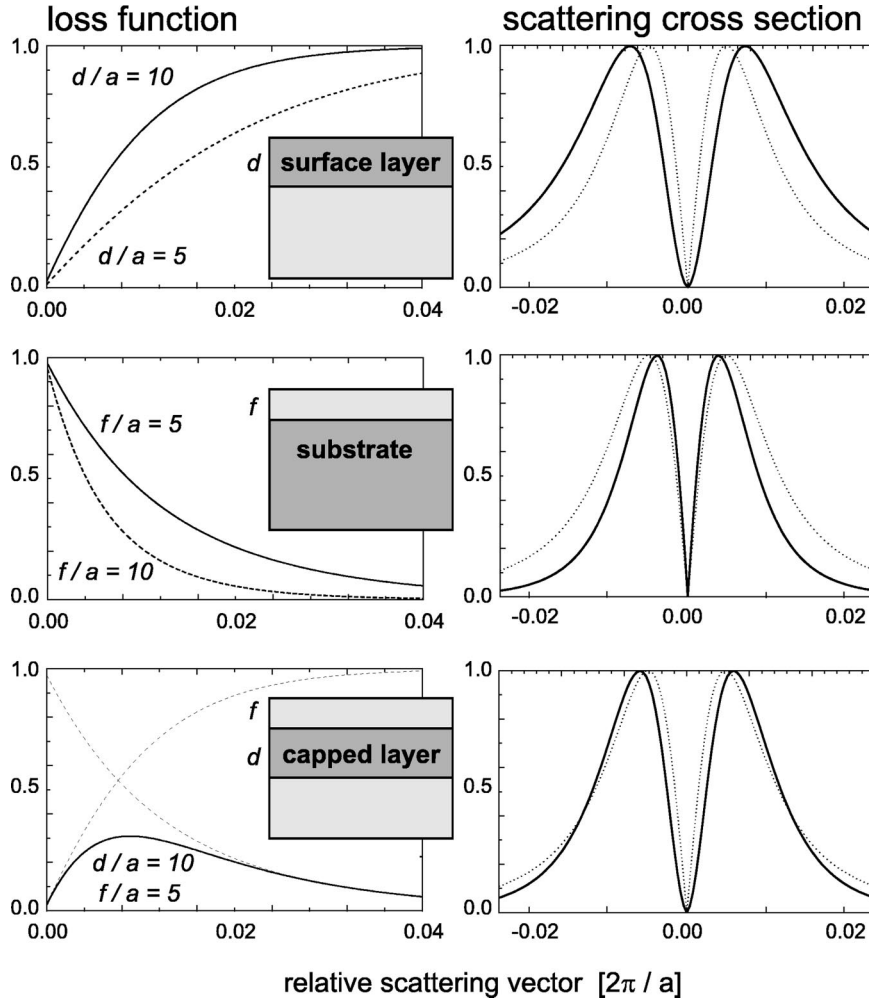


FIG. 1. Simulated loss function (left column) and profile of the dipole scattering cross section (right column) for three different dipole-active (DA) layer configurations: DA surface layer (upper row), DA substrate with dielectric capping layer (middle), and capped DA layer (bottom). The relative scattering vector is given in units of $2\pi/a$ with a as characteristic length, e.g., the monolayer thickness. d and f denote the thickness of dipole-active layer and capping layer, respectively. The scattering profiles are normalized to their maximum. See text for details.

beam is avoided because of tunneling into the substrate.⁹ The well-oriented Ge(001) surfaces (angle of miscut less than 0.15°) and the NaCl films were prepared by standard methods,⁹ including *in situ* sputtering/annealing cycles of the substrate in order to remove any surface contamination, and sublimation of NaCl from an alumina crucible onto the substrate held at a temperature of 200 K (liquid-nitrogen cooling). Annealing the films to 600 K (400 K for films below 1 nm thickness) resulted in sharp LEED patterns from NaCl(001) surfaces. The substrate surface contamination (C, O $\leq 0.5\%$) was monitored using Auger electron spectroscopy.

III. INELASTIC SCATTERING PROFILES OF MULTILAYER SURFACES

The cross section $d^2S/d\Delta E dK_{\parallel}$ for dipole scattering of low-energy electrons at the surface of a layered semi-infinite medium may be separated into a kinematic factor $A(K_{\parallel}, \Delta E)$ independent of the properties of the medium¹⁶ and the loss function $\text{Im}[-1/(\tilde{\epsilon}(q, \omega) + 1)]$.¹⁷ Here K_{\parallel} denotes the surface component of the scattering vector and ΔE the loss energy. The loss function describes the power absorption by the layered surface with $\tilde{\epsilon}(q, \omega)$ as its effective dielectric function depending on energy $\hbar\omega$ and momentum q , respec-

tively. Energy and momentum are conserved in the scattering event, i.e., $\Delta E = \hbar\omega$ and $K_{\parallel} = -q$. In case of normal incidence the following holds for the kinematic factor with v as incident electron velocity (\propto denotes proportionality):

$$A(K_{\parallel}, \omega) \propto \frac{K_{\parallel}}{\left(\frac{\omega^2}{v^2} + K_{\parallel}^2\right)^2}. \quad (1)$$

The profile of the kinematic factor with respect to K_{\parallel} is depicted schematically in the right column panels of Fig. 1 as dotted lines. Here K_{\parallel} is given in units of $2\pi/a$ with a as an arbitrary characteristic length, e.g., the monolayer thickness or the surface lattice constant. The full width at half maximum of the profile scales with $\hbar\omega/\sqrt{E}$ with E as incident electron energy. For the schematic representation in Fig. 1 the ratio v/ω was set to $100/a(\sqrt{3}\pi)$ [corresponding, e.g., to $E = 100$ eV and $\hbar\omega = 0.5$ eV for $a = 0.4$ nm as lattice constant of the NaCl(001) surface].

Calculations of $\tilde{\epsilon}(q, \omega)$ can be based on models of the surface as layered dielectric medium.^{2,3} A closed-form expression of the loss function of a “dipole-active” (DA) semi-infinite substrate capped by a dielectric layer is obtained according to Ref. 3 as

$$\text{Im}\left[\frac{-1}{\tilde{\epsilon}+1}\right] = \frac{2\epsilon_1}{(\epsilon_1+1)^2} \frac{\text{Im}[\Delta]e^{-2|q|f}}{\left(1 + \frac{\epsilon_1-1}{\epsilon_1+1}\text{Re}[\Delta]e^{-2|q|f}\right)^2 + \left(\frac{\epsilon_1-1}{\epsilon_1+1}\text{Im}[\Delta]e^{-2|q|f}\right)^2}, \quad \Delta = \frac{\epsilon_2 - \epsilon_1}{\epsilon_2 + \epsilon_1}, \quad (2)$$

with ϵ_1, ϵ_2 as dielectric constants of the capping layer and the DA substrate, respectively, and f as thickness of the capping layer. In the limits $|q|f \rightarrow \infty$ or $\epsilon_1 \rightarrow 1$ the loss function dependence on q is well approximated as $\exp(-2|q|f)$, which is still a good approximation for $|\epsilon_2|/\epsilon_1 \rightarrow 1$.

Three specific surface models are depicted in cross-sectional view in the left column panels of Fig. 1. One layer is modeled as “dipole-active” (dark gray area) via an oscillator-type dielectric function without dispersion at a single resonance frequency ω_0 .³ The dielectric function of the other layers (light gray area) is assumed to be a real constant around ω_0 . For each surface model [from top to bottom: (i) surface layer, (ii) capped semi-infinite substrate, and (iii) capped layer] the dependence of the loss function on momentum is illustrated schematically in the left column panels of Fig. 1 (calculation for $|\epsilon_2|/\epsilon_1 \rightarrow 1$, normalized).

The simulation of the loss profiles revealed that dispersion of $\tilde{\epsilon}$ can be neglected if damping of the oscillator-type dielectric function is assumed to be high (damping constant of the order of the resonance frequency) in correspondence with the Ge dielectric function in the energy range of interband transitions^{18,19} and our experimental observations. Solid and dashed lines in the viewgraphs for the DA surface layer and the capped DA substrate show the results for different surface layer thicknesses d and capping layer thicknesses f , respectively. The results for the DA surface layer (upper row in Fig. 1) are shown for reference. Since $K_{\parallel}d \rightarrow 0$ in many experimental situations, the exponentially asymptotic dependence of the loss function on K_{\parallel} is usually approximated as proportional to $K_{\parallel}d$.¹⁷ It has been demonstrated experimentally, e.g., for vibrational losses of thin Al_2O_3 films on $\text{Al}(100)$.²⁰

The decrease of the loss function of a DA substrate capped by a dielectric layer of thickness f (center row) with increasing K_{\parallel} is due to screening. The polarization fields of polariton-type interface excitations are attenuated into the dielectric capping layer as $\exp(-|z|/\lambda)$ (Ref. 17) with $\lambda = 2\pi/|q|$ as polariton wave length and z as distance from the interface, resulting in their efficient screening with respect to the vacuum above if $\lambda \leq f$. The loss function simulated for a DA thin layer of thickness $d = 10a$ screened by a capping layer of thickness $f = 5a$ is depicted as solid line in the bottom panel of the left column of Fig. 1. The dotted lines show the loss function of a DA surface layer of thickness $d = 10a$ and of a capped DA semi-infinite substrate of thickness $f = 5a$, respectively, as asymptotes for $q \rightarrow 0$ and $|q| \rightarrow \infty$, respectively.

In combination with the aforementioned kinematic factor (dotted lines in the right column panels) the loss functions which are shown as solid lines in the left column panels of Fig. 1 result in characteristic profiles of the dipole scattering

cross section. Normalized to maximum intensity for better comparison, these profiles are depicted as solid lines in the right column panels for the three surface models, respectively. A DA layer, whether it is at the surface or capped by a dielectric layer, can be recognized by a quadratic dependence of the scattering cross section on K_{\parallel} for $K_{\parallel} \rightarrow 0$. A capping layer, on the other hand, leads to a narrowing of the entire profile. For the DA substrate with a capping layer the full width at half maximum decreases as the thickness of the capping layer increases for fixed $\Delta E/\sqrt{E}$. By choice of the primary energy E the position of the maxima in the kinematic factor with respect to K_{\parallel} may be adjusted for a given ΔE so that specific sections of the loss function can be specifically enhanced in the total cross section. The analysis of the experimental data shown in the following will refer only to the inelastic scattering profile and not to the absolute loss intensity.

IV. RESULTS AND DISCUSSION

Energy loss spectra of the clean Ge(001) surface (lower panel) and of 14 monolayers NaCl on Ge(001) (upper panel), both taken at the $\bar{\Gamma}$ point of the SBZ ($\Delta K_{\parallel} = 0$), are shown in Fig. 2. At the sample temperature of 100 K the clean Ge substrate exhibited a sharp $c(2 \times 4)$ LEED pattern (not shown) due to a buckled dimer row reconstruction²¹ while the surface of the NaCl layer shows no evidence of being reconstructed. Both energy loss spectra in Fig. 2 exhibit loss maxima in the energy range within the NaCl band gap at about 1.4, 2.6, and 5.3 eV, respectively. The peak at 7.85 eV in the upper panel represents scattering due to exciton generation in the NaCl layer.¹⁴

For the clean Ge(001) surface the energy loss maxima at 2.6 and 5.3 eV are reproduced by a simulation of the loss spectrum (dashed lines in the lower panel) based on optical data for the Ge bulk dielectric function. Two sets of experimental data were available for the simulation, one obtained at a temperature of 100 K from ellipsometry data of a Ge(110) surface prepared under UHV conditions¹⁸ (dashed line in the lower panel, experimental reference A) and the other, covering a wider energy range, obtained at room temperature from optical reflectivity data at samples under ambient pressure¹⁹ (dashed-dotted line, experimental reference B). Based on the Ge bulk dielectric function the electron energy loss function was calculated and multiplied by an effective kinematical factor that takes into account the finite momentum resolution of the instrument. The loss at 1.4 eV observed experimentally is not reproduced by the simulations, suggesting that it must be related to surface states. The dashed-dotted line, showing a steep rise of loss intensity above the Ge band gap, exhibits a peak at 1 eV which is not due to a feature of the loss function but is the result of the

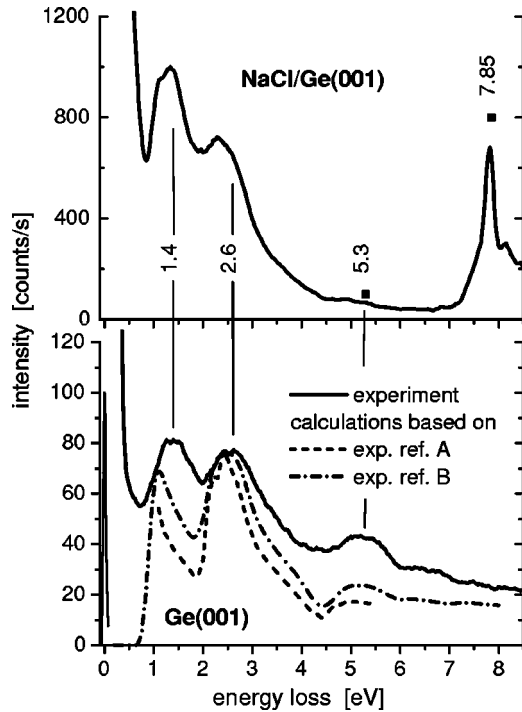


FIG. 2. Lower panel: energy loss spectrum of the clean Ge(001) surface. The dashed line and the dashed-dotted line show simulations based on optical data from experimental reference A (Ref. 18) and B (Ref. 19), respectively. Upper panel: energy loss spectrum of 14 ML NaCl on Ge(001) (primary energy: 64 eV; temperature: 100 K).

effective kinematic factor which decreases as the energy loss increases. The similarity of the loss spectrum of the NaCl-covered Ge(001) surface (upper panel) to that of the clean substrate is only the first evidence that in both spectra the loss features in the NaCl band gap region represent electronic excitations of the substrate. They could also be caused by electron irradiation-induced color centers in and on the NaCl layer, exhibiting electronic transitions in the same energy range.¹⁴

The inelastic scattering profiles for $\Delta E = 2.6$ eV are shown in Figure 3 for different thicknesses of the NaCl layer (3, 6, and 12 ML, respectively). The decrease in profile width with increasing NaCl layer thickness points to an excitation of the NaCl-capped Ge substrate. A quantitative comparison with dipole scattering theory has to take into account the finite momentum resolution, which is limited by surface roughness in our experiment. The NaCl layers accommodate substrate steps by inclined regions,¹¹ leading to a finite terrace width and broadening of the Bragg reflection. Consequently, extraction of the loss function dependence on K_{\parallel} from the experimental inelastic profiles would require a two-dimensional deconvolution with respect to the elastic Bragg profile. For our analysis we have taken an inverse approach. The loss function for a dipole-active Ge substrate [$\epsilon_{Ge}(\hbar\omega = 2.6 \text{ eV}) = 14 + 16i$ (Ref. 18)] with a NaCl capping layer [$\epsilon_{NaCl}(2.6 \text{ eV}) = 2.4$ (Ref. 22)] was calculated with the capping layer thickness f as single free parameter, multiplied with the kinematic factor representing our scattering conditions, and convoluted with the experimental elastic scattering

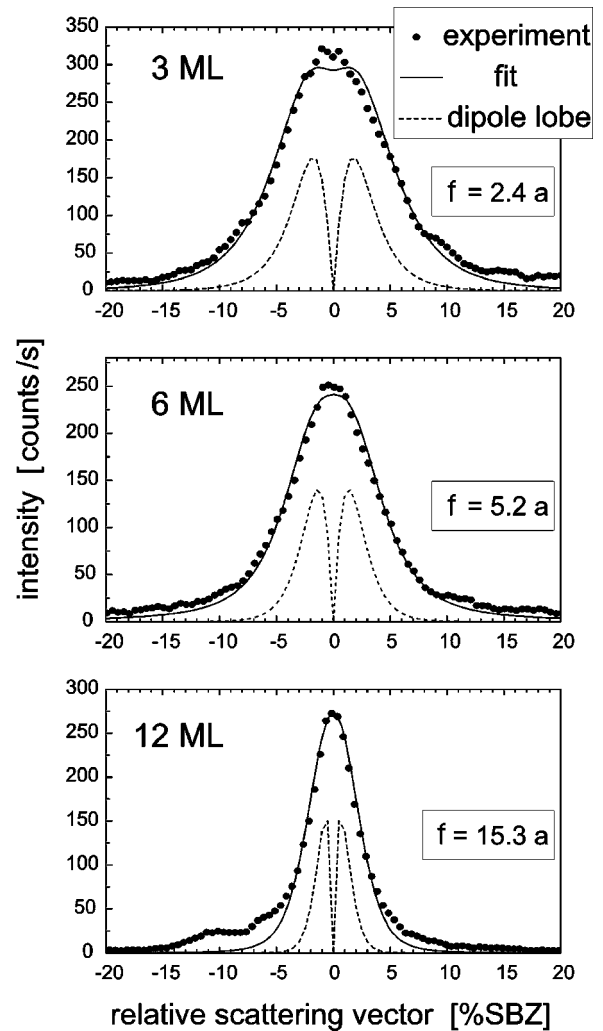


FIG. 3. Angular distribution of inelastically scattered electrons ($\Delta E = 2.6$ eV) around the specular direction. The three panels represent results for 3, 6, and 12 ML NaCl on Ge(001), respectively. Experimental results are shown as scattered curve. The fit according to dipole scattering theory is shown as solid line. Dashed curves represent the dipole lobe as calculated by the fitting procedure before convolution with the elastic diffraction spot profile. f represents the film thickness in monolayers as calculated by the fitting procedure.

profile (i.e., for $\Delta E = 0$) measured for the same primary energy. That calculated dipole scattering cross section was fitted iteratively to the experimental inelastic profiles by variation of f . The results are given in Fig. 3 in units of the NaCl monolayer thickness $a = 0.28$ nm. The corresponding fits denoted by solid lines in Fig. 3 provide a nearly perfect match with experiment. The characteristic dip of the kinematic factor for $K_{\parallel} \rightarrow 0$ is not resolved in the experiment. The dashed lines in Fig. 3 represent the calculated inelastic scattering profile before convolution.

Up to a capping layer thickness of 12 ML, we find a very good agreement of f with the capping layer thickness determined by the amount of deposited NaCl which was measured by a quartz microbalance calibrated via LEED oscillations. The results for all measured thicknesses are summarized in

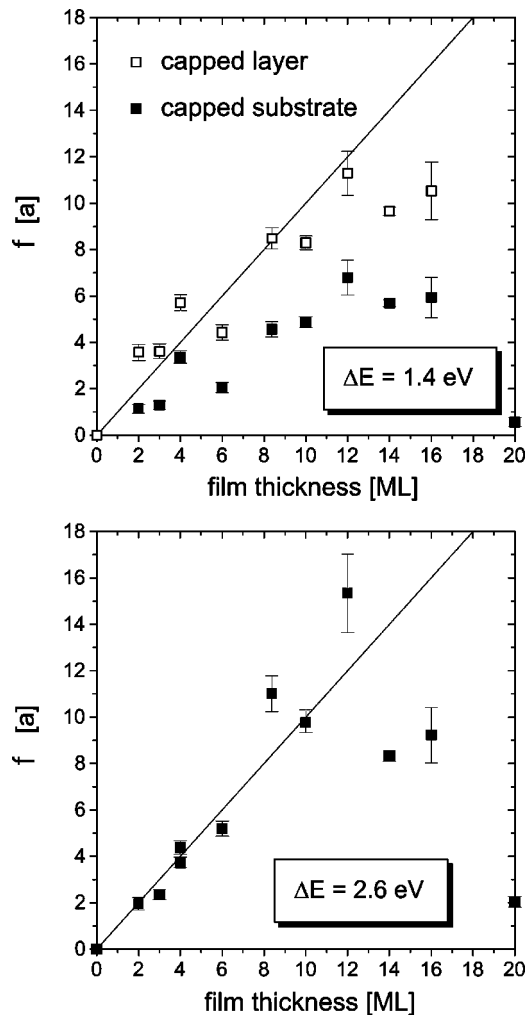


FIG. 4. Value f as calculated by the fitting procedure in comparison with the actual film thickness. The lower panel shows the results for $\Delta E = 2.6 \text{ eV}$, assuming an interface mode of the semi-infinite Ge substrate. The upper panel shows the results for $\Delta E = 1.4 \text{ eV}$ assuming a dipole-active substrate (filled boxes) or a dipole-active interface layer (open boxes).

the lower panel of Fig. 4. For film thicknesses larger than 13 ML the width of the inelastic profiles increases with film thickness in connection with a dramatic decrease of total loss intensity, pointing to a perfect screening of the substrate. Other excitations, probably of low-density color centers in the NaCl layer, then becoming prominent in the loss spectrum, can already be seen at the base of the dipole lobe of 12 ML NaCl/Ge(001) (see Fig. 3). Prolonged electron irradiation leads to more significant energy losses in the regime 1.2–2.7 eV due to surface color centers.¹⁴ Their profiles in momentum space (not shown here) are independent of NaCl layer thickness and in perfect agreement with the model of a thin dipole-active surface layer.

A similar analysis was performed for profiles of the energy loss of 1.4 eV which was not reproduced by Ge optical data. While the profile width also decreases with increasing NaCl film thickness, the fit for the dipole-active substrate model yields f constantly as too low compared to the measured NaCl layer thickness (see filled squares in the upper

panel of Fig. 4). Calculations for a dipole-active capped layer, however, provide a good fit to the experimental data with f in the range of the actual film thickness (open squares). As first approximation to the loss function we chose $(1 - \exp[-2K_{\parallel}d]) \times \exp[-2K_{\parallel}f]$ with d and f as thickness of the dipole-active layer and the capping layer, respectively. A consistent fit of all data was obtained when fixing $d = 1 \text{ nm}$. The uncertainty of d , however, is within an order of magnitude as we estimate from fixing f to the actual value, i.e., the measured NaCl layer thickness, and fitting d . As can be seen from Fig. 1, the loss function is affected by the actual thickness d of the dipole-active layer at the Ge interface especially in the limit $K_{\parallel} \rightarrow 0$ so that the finite momentum resolution due to surface defects becomes crucial. The angular distribution of the inelastic scattering clearly shows that the origin of the energy loss at about 1.4 eV must be located at the Ge surface or NaCl/Ge interface, respectively. Dimerization-induced surface states on Ge(001) have been identified by angle-resolved photoemission^{23–26} and inverse photoemission experiments²⁵ in combination with band structure calculations.²⁴ For the (2×1) -reconstructed Ge(001) surface at room temperature the surface band gap has been determined by Kipp *et al.* as about 1 eV at $\bar{\Gamma}$ and 1.9 eV at \bar{J} ,²⁵ with the filled and unfilled states being located at the dimer dangling bonds. It has been demonstrated that the energetic position of the filled dangling bond state $E(D_{UP})$ does not change during the $(2 \times 1) \rightarrow c(2 \times 4)$ phase transition below room temperature.²⁶ Especially at $\bar{\Gamma}$, however, the experimental results for $E(D_{UP})$ vary from 0.6 eV below the valence-band maximum (VBM)²³ to 0.27 eV above VBM as observed by Kipp *et al.*²⁵ This may be due to a narrow metallic surface state band ascribed to disorder-induced defects²⁷ which disappears for temperatures below the $(2 \times 1) \rightarrow c(2 \times 4)$ phase transition. Consequently, for a $c(2 \times 4)$ -reconstructed Ge(001) at a temperature of 120 K we take 1 eV as a lower limit for the surface band gap and interpret the energy loss observed at 1.4 eV in our experiments as linked to electronic transitions between the dangling bond filled and empty states.

The observation that the intensity of the energy loss at 1.4 eV at $\bar{\Gamma}$ prevails after deposition of several monolayers of NaCl indicates that the Ge dimers remain intact at the NaCl/Ge interface and their electronic states are essentially unaltered by the NaCl layer. Surface dimer bonds are in fact quite strong with a binding energy of $\geq 1 \text{ eV}$ and it has been demonstrated by photoelectron spectroscopy that even for alkali metal adsorption on Si(001) the Si surface dimers remain intact.²⁸ In the case of K/Si(001) and Cs/Si(001) the alkali metals bond covalently to the silicon dimers, shifting the energy of the filled dangling bond states by 0.1–0.5 eV. Compared to the alkali metal–Si(001) bonds we expect the bonds between a NaCl layer and the Ge(001) surface dimers to be rather weak because the valence-band maximum of the NaCl layer is located about 4 eV below the valence-band maximum of the Ge substrate as shown by photoelectron spectroscopy.¹⁰ Being located in the middle of the NaCl band gap the dimer dangling bond states lack adequate partners for chemical bonds.

While the character of bonding between NaCl and

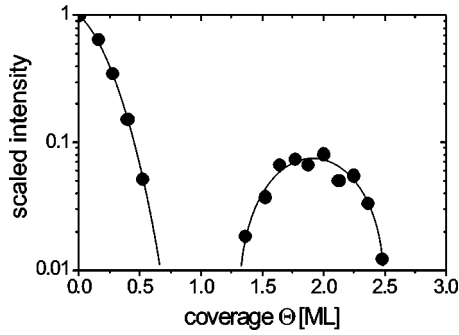


FIG. 5. Intensity of half-order LEED spots of the NaCl/Ge(001) depending on NaCl coverage.

Ge(001) is still subject to debate, its weakness in relation to ionic bonds within NaCl is manifested by the carpet growth mode of NaCl on Ge(001) which, close to substrate steps, minimizes the electrostatic energy within the NaCl layer at the cost of binding energy between the NaCl layer and the Ge substrate.¹¹ The average loss of binding energy between the NaCl layer and the Ge substrate has been estimated by the size of inclined regions of the NaCl “carpet” at Ge steps as 0.13 eV per surface Ge atom. Taking into account the weak coupling between the dimer dangling bond states and the NaCl valence electrons and the relatively weak bonding between NaCl and Ge substrate observed experimentally, it seems reasonable that the Ge dimers rest intact at the interface, exhibiting electronic filled and empty states which remain essentially unaltered while their energy may be slightly shifted due to polarization induced by the overlayer.

Support for the assumption that the dimerization is not removed is provided by x-ray investigations of the NaCl/Ge(001) interface, showing a (2×1) reconstruction of the NaCl/Ge(001) interface up to a thickness of the covering NaCl layer up to 9 ML,²⁹ and by our LEED data. While LEED is insensitive to the interface for NaCl coverages higher than a few monolayers we find a recurrence of (2×1) superstructure spots during NaCl epitaxy when the first two NaCl monolayers are completed. The intensity of half-order spots plotted versus NaCl coverage, showing a recurrence of the spots at the completion of a double layer, is observed in Fig. 5. The intensity was taken from LEED profiles in the $[110]$ direction (Fig. 6), comprising the specular reflection at 0% SBZ and half-order positions at 50% and -50% SBZ, respectively. While the recurrence of the half-order spots is difficult to see in Fig. 6, intensity oscillations of the specular spot with increasing NaCl coverage are clearly visible. The oscillations were used for calibrating the NaCl coverage. Scanning tunneling microscopy (STM) measurements confirm that growth occurs via an initial double layer followed by atomic single layers.³⁰ STM does not show a (2×1) reconstruction of the NaCl layer surface so that the NaCl/Ge interface must be the origin of the LEED observation.

The role that inclined regions of the NaCl carpet at Ge steps play for the occurrence of the observed energy loss at 1.4 eV will be elucidated in future experiments on Ge substrates of various standard miscut angles. On the low-miscut

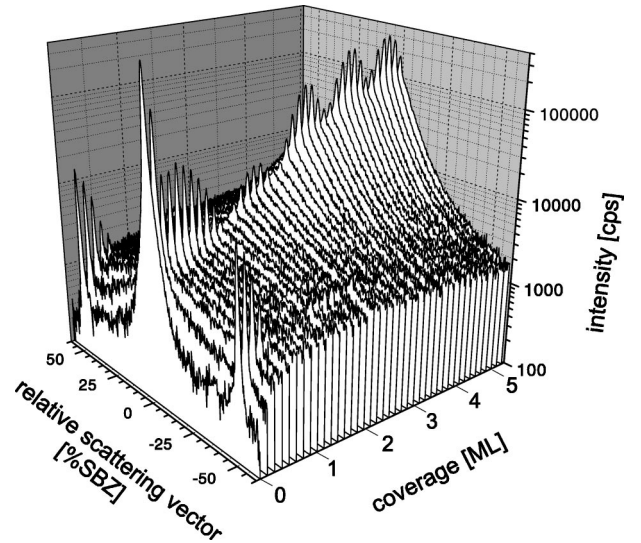


FIG. 6. LEED profiles in $[110]$ direction taken for increasing NaCl coverage at a temperature of 200 K. The profiles comprise the specular spot (0% SBZ) and half-order positions (50%, -50% SBZ).

(001) substrates used in the experiments presented here, the intensity of the 1.4 eV loss at $\bar{\Gamma}$ does not appear to be reduced with increasing NaCl coverage when related to the energy loss intensities of Ge bulk interband transitions (see Fig. 2). Therefore we assume that the entire interface, and not only areas close to Ge substrate steps, contributes to the energy loss at 1.4 eV.

The angular distribution of the inelastic scattering at 5.3 and 7.85 eV energy loss have not been demonstrated here. As shown elsewhere, the excitation mechanism is not purely dipolar in character so that the dielectric model depicted here cannot be applied.¹⁴

V. CONCLUSION

We have experimentally demonstrated that a high-resolution analysis of the angular distribution of inelastic dipole scattering may support the interpretation of energy loss spectra in the range of electronic interband transitions by providing unequivocal information on the excitation of buried dipole-active layers. For the NaCl/Ge(001) system we find losses due to substrate excitations for NaCl surface layer thicknesses up to 12 ML. Identification of the energy loss at 1.4 eV as due to electronic interband transitions localized at the NaCl/Ge(001) interface provides evidence that the substrate dimerization is not removed at the NaCl/Ge interface.

We expect the analysis to work well for insulating capping layers with relatively low dielectric constants. Screening of metallic or semiconducting overlayers ($\epsilon \gg 1$, see equation) will reduce the total loss intensity significantly while its effect on the profile depends on the ratio $|\epsilon_2|/\epsilon_1$. For $|\epsilon_2|/\epsilon_1 \rightarrow 1$ the loss function of a capped dipole-active substrate may be approximated as proportional to $\exp[-2K|d|]$. Considering a capped dipole-active layer of finite thickness like, e.g., a space-charge layer at the interface

of a semiconducting substrate to a dielectric surface layer, the loss function is expected to exhibit a maximum for a finite wavelength because the short-wavelength components are effectively screened by the capping layer and the long-wavelength components are effectively attenuated by the finite thickness of the dipole-active layer. High-resolution measurements of the inelastic scattering profiles for different ratios $\Delta E/E$ should render possible to extract the depen-

dence of the loss function on K_{\parallel} in detail. Studies with semiconducting and conducting films are in progress.

ACKNOWLEDGMENTS

We gratefully acknowledge valuable discussions with H. Pfnür. Financial support was provided by Deutsche Forschungsgemeinschaft.

*Electronic address: zielasek@fkp.uni-hannover.de URL: <http://www.fkp.uni-hannover.de>

¹R. Camley and D. Mills, Phys. Rev. B **29**, 1695 (1984).

²P. Lambin, J. Vigneron, and A. Lucas, Phys. Rev. B **32**, 8203 (1985).

³P. Lambin, J. Vigneron, and A. Lucas, Comput. Phys. Commun. **60**, 351 (1990).

⁴P. Thiry, M. Liehr, J. Pireaux, and R. Caudano, J. Vac. Sci. Technol. B **4**, 1028 (1986).

⁵T. Tsuruoka, Y. Uehara, S. Ushioda, T. Kojima, and Y. Sugiyama, Surf. Sci. **368**, 185 (1996).

⁶V. Polyakov, A. Elbe, J. Wu, G. Lapeyre, and J. Schäfer, Appl. Surf. Sci. **104/105**, 24 (1996).

⁷C. Lohe, A. Leuther, A. Förster, and H. Lüth, Phys. Rev. B **47**, 3819 (1993).

⁸M. Liehr and P. Thiry, J. Electron Spectrosc. Relat. Phenom. **54/55**, 1013 (1990).

⁹S. Fölsch, U. Barjenbruch, and M. Henzler, Thin Solid Films **172**, 123 (1989).

¹⁰S. Fölsch, Ph.D. thesis, University of Hannover, 1991.

¹¹C. Schwennicke, J. Schimmelpfennig, and H. Pfnür, Surf. Sci. **293**, 57 (1993).

¹²U. Malaske, C. Tegenkamp, M. Henzler, and H. Pfnür, Surf. Sci. **408**, 237 (1998).

¹³C. Tegenkamp, H. Pfnür, W. Ernst, U. Malaske, J. Wollschläger, D. Peterka, K. Schröder, V. Zielasek, and M. Henzler, J. Phys.: Condens. Matter **11**, 9943 (1999).

¹⁴V. Zielasek, T. Hildebrandt, and M. Henzler, Phys. Rev. B **62**, 2912 (2000).

¹⁵H. Claus, A. Büssenschütt, and M. Henzler, Rev. Sci. Instrum. **63**, 2195 (1992).

¹⁶B. Persson and J. Demuth, Phys. Rev. B **30**, 5968 (1984).

¹⁷H. Ibach and D. Mills, *Electron Energy Loss Spectroscopy and Surface Vibrations* (Academic Press, New York, 1982).

¹⁸L. Viña, S. Logothedidis, and M. Cardona, Phys. Rev. B **30**, 1979 (1984).

¹⁹H.R. Philipp and M. Cardona, Phys. Rev. **129**, 1550 (1963).

²⁰A. Büssenschütt, H. Claus, and M. Henzler, Phys. Rev. B **49**, 7829 (1994).

²¹S. Kevan, Phys. Rev. B **32**, 2344 (1985).

²²*Physics of Color Centers*, edited by W. Fowler (Academic Press, New York, 1968).

²³J. Nelson, W. Gignac, R. Williams, S. Robey, J. Tobin, and D. Shirley, Phys. Rev. B **27**, 3924 (1983).

²⁴E. Landemark, R. Uhrberg, P. Krüger, and J. Pollmann, Surf. Sci. **236**, L359 (1990).

²⁵L. Kipp, R. Manzke, and M. Sibowski, Surf. Sci. **269**, 854 (1992).

²⁶A. Laine, M. SeSeta, C. Cepek, S. Vandre, A. Goldoni, N. Franco, J. Avila, M. Asensio, and M. Sancrotti, Surf. Sci. **402-404**, 871 (1998).

²⁷S. Kevan and N. Stoffel, Phys. Rev. Lett. **53**, 702 (1984).

²⁸Y. Enta, T. Kinoshita, S. Suzuki, and S. Kono, Phys. Rev. B **39**, 1125 (1989).

²⁹C. Lucas, G. Wong, C. Dower, and F. Lamelas, Surf. Sci. **286**, 46 (1993).

³⁰K. Glöckler, M. Sokolowski, A. Soukopp, and E. Umbach, Phys. Rev. B **54**, 7705 (1996).